

Mesh Sensitivity Analysis for the Numerical Simulation of a Damaged Ship Model

Ivana Martić¹, Nastia Degiuli¹, Andrea Farkas¹, Josip Bašić²

¹ Faculty of Mechanical Engineering and Naval Architecture, University of Zagreb,
Zagreb, Croatia

² Faculty of Electrical Engineering, Mechanical Engineering and Naval Architecture, University of Split,
Split, Croatia

ABSTRACT

In this paper, a numerical simulation of a damaged ship model is investigated. The damaged ship model has a hole that involves eight subspaces of the cargo tank between two watertight transverse bulkheads. The damage of the ship bottom, possibly due to grounding, amounts to 20% of the total length of the ship. In this paper, the numerical simulation of flow around the hole and inside the tanks and a calculation of the total resistance of the damaged model are carried out using the commercial software package STAR-CCM+. The mathematical model is based on the Reynolds Averaged Navier-Stokes (RANS) equations, with the Volume of Fluid (VOF) method for two-phase turbulent flow, and the $k-\epsilon$ turbulence model. The mesh sensitivity analysis of the results obtained for the total resistance force of the damaged model is conducted using different mesh resolutions. The numerical results of the total resistance force of the damaged model are compared to the experimental results.

KEY WORDS: Computational Fluid Dynamics (CFD), Reynolds Averaged Navier-Stokes (RANS) equations, Volume of Fluid (VOF) method, turbulent two-phase flow, damaged ship model

INTRODUCTION

A ship after a maritime accident, e.g. grounding or collision, often loses the ability of self-propulsion due to mechanical breakdown, and thus needs to be towed to a safe location before losing stability or structural integrity. The towing often has to be performed despite rough weather conditions and in limited time. In order to ensure the safety of the towing operation, it is necessary to calculate all the forces and loads that act on the ship hull during the tow. On the other hand, if the ship manages to maintain its ability to advance using its self-propulsion system despite the damage that occurred, it is necessary to determine the total resistance force acting on the ship hull. Ship stability and seakeeping characteristics are different in the damaged condition as is the total resistance force due to the increased draught resulting as compensation for the displacement loss. The flow around the damage hole and the fluid motions inside the flooded compartments may cause severe motions coupled with ship global motions and a significant increase in the total resistance force. In order to take the viscous effects of progressive flooding into account, CFD based on viscous flow theory is often used. The RANS equations enable the simulation of

possible violent flows with a non-linear free surface inside the flooded compartments, and take into account the impact of the inner compartment geometry and the size/shape of the damage hole on hydrodynamic forces and ship motions. The VOF method has become one of the most commonly used methods for free surface flow calculations.

Since different damage scenarios cause specific damage on a ship hull, experimental tests are often conducted and are believed to provide reliable results. However, experimental tests of damaged ship models may involve many sources of uncertainties that are hard to control and evaluate, which makes the CFD validation in this case questionable. Thus, experimental tests of damaged ship motions and loads are performed in order to develop a valuable CFD database (Lee et al., 2012; Lee et al., 2016). Experiments conducted for this purpose have to be designed and prepared in such a way that the uncertainty factors are eliminated as far as possible. Lee et al. (2016) conducted several experimental tests in order to collect data for CFD solver validation both in intact and damaged ship conditions, at two different wave heading angles. Their damaged compartments had simple geometry and ventilation holes as well as a mooring system to prevent drift forces and parametric roll. On the other hand, Lee et al. (2012) also discovered that flow in their asymmetrically placed damaged compartment in the midship area may act as an anti-rolling tank, interfering with the roll motion of the ship. Wood et al. (2010) predicted the floodwater flow through different damage hole geometries in relation to the size of the flooded compartment. Gao et al. (2009, 2011) focused their research on floodwater dynamics and their influence on ship motions based on the VOF method. Guo et al. (2013) conducted the verification and validation of ship resistance force and the flow field obtained by numerical simulations using the KVLCC2 tanker. In their experimental setup, the vessel was divided into three segments and resistance was measured separately. They concluded that the turbulence model has a large impact on the prediction of the resistance force when it comes to the flow at the aft part of the hull. Yang et al. (2009) investigated the resistance and self-propulsion of the damaged ship in various damage scenarios with high uncertainty of the experimental tests. They noticed that higher propulsion power is required in the case of bow trim and that the numerical results are in good agreement with the measured experimental data.

In this paper, the total resistance force of the damaged ship is obtained with the commercial CFD software package STAR-CCM+ using a finite volume method (FVM) and a VOF interface capturing method, by solving RANS equations. The $k-\epsilon$ turbulence model is used and the

results obtained by numerical simulations are compared to the experimental data for four different speeds. Three different mesh densities were used for the fluid domain discretization. The damage is simulated as a grounding scenario based on statistical data, and involves a maximum of eight flooded compartments between two watertight bulkheads. Additionally, flow inside the flooded compartments and around the hole is investigated.

NUMERICAL MODEL

Fluid flow is modelled using the discrete finite volume method (FVM) representation of RANS and continuity equations. The continuity and momentum equations for incompressible flow in the Cartesian coordinate system are given as follows (Ferziger and Perić, 2002):

$$\frac{\partial(\rho\bar{u}_i)}{\partial x_i} = 0 \quad (1)$$

$$\frac{\partial(\rho\bar{u}_i)}{\partial t} + \frac{\partial}{\partial x_j} (\rho\bar{u}_i\bar{u}_j + \rho\bar{u}'_i\bar{u}'_j) = -\frac{\partial\bar{p}}{\partial x_i} + \frac{\partial\bar{\tau}_{ij}}{\partial x_j} \quad (2)$$

where ρ is the fluid density, \bar{u}_i is the averaged Cartesian components of the velocity vector, $\rho\bar{u}'_i\bar{u}'_j$ is the Reynolds stress, and \bar{p} is the mean pressure. $\bar{\tau}_{ij}$ is the mean viscous stress tensor as follows:

$$\bar{\tau}_{ij} = \mu \left(\frac{\partial\bar{u}_i}{\partial x_j} + \frac{\partial\bar{u}_j}{\partial x_i} \right) \quad (3)$$

where μ is the dynamic viscosity.

In the RANS equations, instantaneous velocity and pressure fields are decomposed into a mean value and a fluctuating component.

The k - ϵ turbulence model is used to model the Reynolds stress tensor in terms of the mean flow quantities as a function of the turbulence kinetic energy and dissipation of that energy, which modifies the calculation of the viscous stress tensor by utilizing the turbulent eddy viscosity μ_t . It includes two extra transport equations to represent the turbulent properties of the flow. The k - ϵ turbulence model is commonly used for industrial applications since it shows good agreement with the experimental results and reduces the required CPU time to perform calculations (Querard et al., 2008).

The VOF method is used to capture the free surface, creating the additional transport equation solved for the volume fraction:

$$\frac{\partial}{\partial t} \alpha + \nabla \cdot (\alpha u_i) = 0 \quad (4)$$

where the volume fraction of the phase in a computational cell α is 0 for air and 1 for water, and the sharp gradient around the value 0.5 denotes the free surface. This allows the modelling of two fluids as a single fluid whose physical characteristics calculated in each computational cell depend on the volume fraction of the phase. The same governing equations are solved for a single-phase problem, as well as for the multi-phase problem within the computational domain.

Mesh preparation and simulation setup

Mesh is prepared based on imported NURBS surfaces of the model hull, deck and fluid domain. All boundary surfaces of the domain are placed at a length of L_{pp} away from the ship model aft, fore part and free surface. Hexahedral unstructured mesh with prismatic boundary layers is created using the “Automated Mesh” operation within the STAR-CCM+ software package (CD Adapco, 2016). Trimmed mesh is used and one half of the domain is modelled considering the

symmetrical flow around the symmetrically damaged hull. The mesh quality is evaluated by inspecting the values of the wall y^+ parameter and the convective Courant number during the simulations.

Pressure and velocity boundary conditions are imposed on the domain boundaries, and a wall boundary condition is imposed on the model hull. Volumetric mesh refinements are made in the fore and aft part of the hull, inside the flooded tanks, and around the bottom hole. Free surface mesh refinements are also made in order to properly catch the Kelvin wake angle around and behind the hull. The total thickness of the boundary layer is defined for each considered ship model speed, based on two wall functions in order to keep the y^+ value around 50:

$$y^+ = y \text{ } Rn \sqrt{\frac{C_f}{2}} \frac{1}{L_{pp}} \quad (5)$$

$$y^+ = 0.172 \left(\frac{y}{L_{pp}} \right) Rn^{0.9} \quad (6)$$

where y is the total thickness of the boundary layer, C_f is the frictional resistance coefficient, and Rn is the Reynolds number.

Volumetric mesh that consists of about 5.2 million cells is shown in Fig. 1 and the tank area refinements are shown in Figs. 2 and 3. The cell size of the mesh around the damage hole and flooded tanks amounts to 12.5% of the base size. In the sharp corners of the rectangular flooded tank, the prism layer is retracted and significantly thinner. The total thickness of the prism layer according to the wall functions is set differently for each considered Froude number. The number of prismatic layers is set at 6 and the prism layer stretching factor is set at 1.5. The base cell size of the mesh containing a total of about 3.4 million cells is set at 0.055 m, and that of the mesh containing a total of about 5.2 million cells is set at 0.045 m. The base size of the coarse mesh containing a total of about 2.2 million cells is set at 0.07 m.

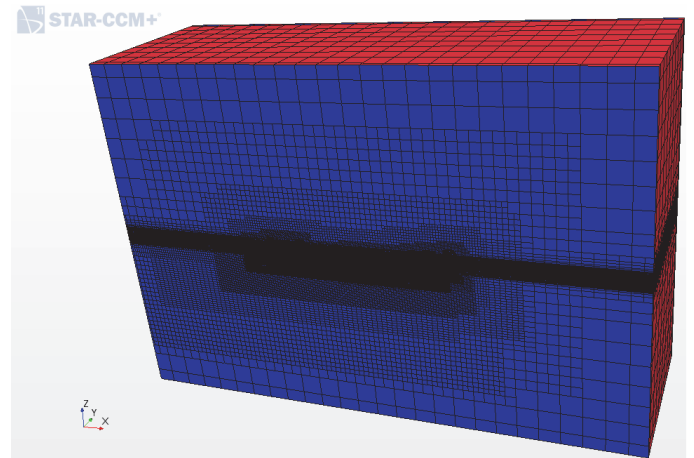


Fig. 1 Fine mesh of the damaged hull model

The water characteristics are set in accordance with the measured environmental conditions during the towing procedure in the experimental tank, conducted in *Brodarski Institute* (Brodarski Institute, 2015). In order to calculate the pressure field and couple it to the velocity field, a segregated flow model is used to solve the conservation equations for each Eulerian phase. The solution algorithm uses the SIMPLE-type approach, which has separate pressure and velocity solvers. An implicit unsteady solver is used to control the update at each physical time. A second-order “Upwind Differencing Scheme” is used so that higher-order accuracy is achieved. For temporal discretization, the first-order temporal scheme is used, which

is also referred to as Euler Implicit.

The linearized system of equations is solved within inner iterations using the Algebraic Multigrid (AMG) solver where the coarse level equations are generated without any use of the geometry or remeshing of the coarse levels. The advantage of the AMG solver is that no coarse level grids have to be generated or stored, which makes the AMG solver appropriate and useful for use on unstructured meshes. Ten inner iterations were used within all simulations.

The hydrostatic pressure and velocity field of VOF waves are defined as field functions as well as a volume fraction of phase α . In order to avoid wave reflections from the domain boundaries, the VOF wave damping parameter is defined through the following equation:

$$dvar \approx \frac{L_{pp}}{2} + \frac{L_{pp}}{2} \cos^2 \left(\frac{\pi}{2} \frac{t}{10T} \right) \quad (7)$$

where T is the time required for the fluid to exceed the model length depending on the ship model speed. Generated waves are damped in the entire calculation domain from the beginning of the simulation. When t reaches $10T$, the damping domain is reduced by about half of its size. The larger damping domain fastens the convergence of the results at the beginning of the simulation.

The VOF sharpening factor is set at 0.5 in order to reduce the numerical diffusion of the free surface.

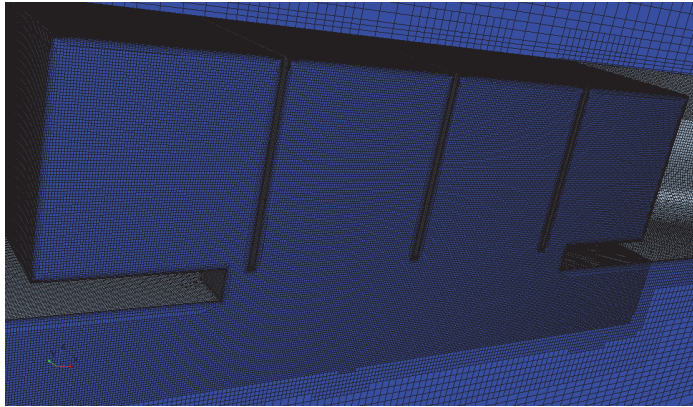


Fig. 2 Mesh refinement of the damage hole and flooded tanks

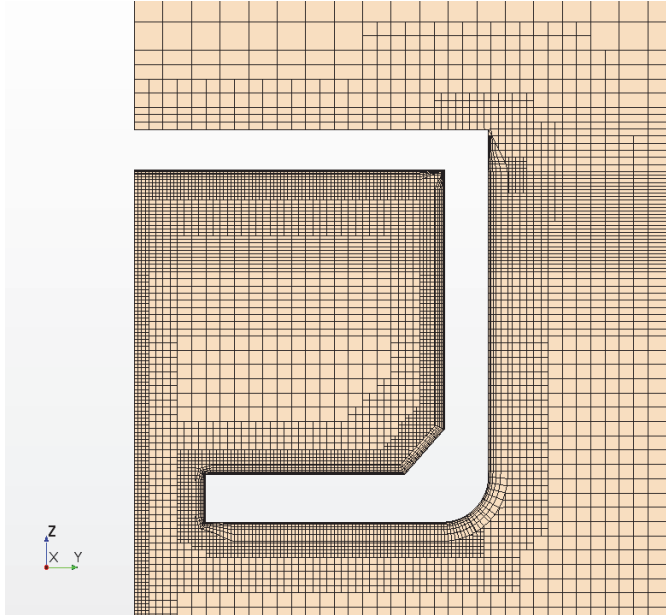


Fig. 3 Cross section of the mesh refinement of the flooded tank

Experimental setup

A Panamax size double hull tanker model was made of plywood at a scale of 1:29, and was towed in the *Brodarski Institute*, Zagreb, in an intact and in a damaged condition (Brodarski Institute, 2015). The total resistance force was measured for various Froude numbers in 24 experiments for the intact, and 6 experiments for the damaged model. The body plan of the ship model is shown in Fig. 4 and the main characteristics of the damaged model and experimental setup are given in Table 1.

Experiments with the damaged model were conducted in calm water for six Froude numbers in a range from 0.073 to 0.135. Three different Froude numbers are considered within the CFD simulation in this paper and the obtained results are compared with the experimental data. The size and the position of the damage hole in the double hull of the tanker are determined based on the statistical data of ship grounding accidents (Marine Environment Protection Committee, 2003) and the Monte Carlo simulation. Based on the obtained results, the maximum possible damage included eight flooded compartments between two watertight bulkheads. The damage hole in the bottom is 20% of the full breadth and extends between frames #110 and #148, i.e. 20% of the hull length, which is schematically depicted in Fig. 5. The damage hole has a rectangular shape and is symmetrically placed in the hull midship area. The hole is properly scaled and applied to the tanker model in order for experiments to be performed on the increase of the total resistance force due to fluid motions inside the tanks and inflow/outflow of the fluid through the hole.

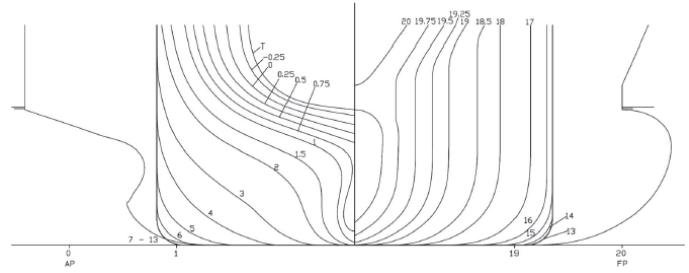


Fig. 4 Body plan of the ship model

Table 1. Main characteristics of the damaged model and experimental setup data

	Damaged model
Length on waterplane L_{WL} , m	6.2009
Length between perpendiculars L_{PP} , m	6.0667
Breadth B , m	1.1176
Block coefficient C_B	0.80
Midship coefficient C_M	0.995
Draught, aft T_A	0.451
Draught, forward T_F	0.472
Trim t , m	-0.02
Wetted surface S , m^2	10.484
Displacement volume V , m^3	2.5616
Water temperature, $^{\circ}C$	22.5
Towing tank dimensions $L \times B \times D$, m	276.3 x 12.5 x 6.0

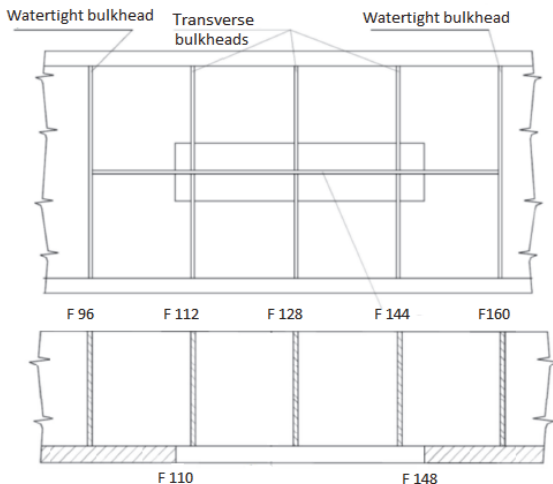


Fig. 5 The damage hole in the horizontal (upper figure) and transversal section (lower figure)



Fig. 6 Towing procedure of the damaged model



Fig. 7 The damage hole in the bottom

The flooded compartments are divided by one longitudinal bulkhead and three transversal bulkheads. Each flooded tank due to the hole in the bottom has a ventilation pipe at the top of the tank covered with transparent plexiglas which allowed air flow without affecting the water flow inside the tanks. The damaged tanker model during the experiment can be seen in Fig. 6 and the damage hole in the bottom can be seen in Fig. 7.

Bašić et al. (2017) compared the total resistance results obtained using CFD with experimental data for the intact as well as for the damaged model and found good agreement between the results considering the uncertainty of the measured values due to the unsteady flow effects that occur near the damage hole and inside the tank as was found during the numerical simulations. CFD simulations using moderately refined mesh showed that the flow inside the tanks was somewhat modified by the presence of the transverse bulkheads. On the edges and corners of the

damage hole in the bottom, large pressure gradients were noticed, i.e. cavity flow occurred in each tank opening causing oscillations of the force acting on the tank wetted surface areas. Due to these unsteady flow effects, the steady flow convergence was prolonged and the total resistance force had convergence issues. The solution to this problem was an increase in the time step after the resistance force acting on the model hull, but excluding the force acting on the tanks, had converged.

RESULTS

The aim of this research was to analyze the effect of the unstructured mesh density on the results for the total resistance force of the damaged model towed in calm water. As already mentioned, three various mesh densities were used within the mesh sensitivity analysis. The results obtained by the fine mesh M3 containing 5.2 million cells show good agreement with the experimental data, as can be seen in Tables 2 and 3. The total resistance force converged to a steady value with sufficiently low residuals. Considering the computational resources of a personal computer and the required computational time, calculations performed using the mesh with a higher number of cells would significantly prolong the required computational time. On the other hand, using coarse mesh M1 with 2.2 million cells as well as medium mesh M2 with 3.4 million cells led to some convergence issues. A steady force could not be obtained due to the unsteady flow in the flooded tanks. Due to the complex and sharp geometry around the bottom hole and around the transverse bulkheads, high pressure gradient areas occur which led to the formation of vortices. These unsteady flow effects caused an oscillation of the numerically obtained results in the case of the coarse and medium mesh.

Considering the high oscillations of the total resistance force, the numerically obtained results using coarse and medium mesh densities are mean values of the total resistance force based on the last 20% of the total physical time.

In Fig. 8, the numerically obtained results are graphically compared to the experimental data measured in *Brodarski Institute*.

The results obtained during the experiment in the towing tank for the same tanker model in the intact condition can also be seen in Fig. 8 (Brodarski Institute, 2015). The results of the relevant part of the examined Froude number range are presented in Fig. 8. The total resistance force of the intact model in calm water obtained using STAR-CCM+ shows very good agreement compared to the experimental data (Farkas, 2016). The simulation setup of the total resistance force in calm water in the case of the damaged model is similar to that of the intact model (Farkas, 2016).

In the damaged condition, for the Froude number 0.073, good agreement between the experimental and numerical results is obtained using the fine mesh M3. The total resistance force for the same Froude number, obtained using the coarse mesh M1, shows significant under-prediction of the results. In the case of the Froude number 0.099, the smallest relative error is obtained using the medium mesh M2. For the same Froude number, results obtained using the coarse mesh M1 compared to the medium mesh M2 show smaller deviation in comparison with the experimental results. However, the results obtained using mesh M1 and M2 cannot be taken as completely relevant in the verification and validation procedure considering the relatively high oscillations of the results. Relative errors of the obtained numerical results are calculated using the following equation:

$$\text{relative error [\%]} = \frac{R_{T,CFD} - R_{T,EXP}}{R_{T,EXP}} \cdot 100 \quad (8)$$

The relative error of the numerically obtained total resistance force is between 2% and 12.5% for the coarse mesh M1, between 3% and 3.5% for the medium mesh M2, and between 0.05 and 1.5% for the fine mesh M3.

High oscillations of the results could be reduced, i.e. a steady resistance force could be achieved by increasing the time step in each simulation after the total resistance force acting on the model hull, but excluding the force on the tanks, reaches a steady value (Bašić et al., 2017). In this way, the unsteady flow effects around the damage hole and transverse bulkheads could be numerically skipped. Obviously, sufficiently small cell dimensions, e.g. for the mesh M3, inside tanks, and in the boundary layer of the tank walls, lead to a steady resistance force despite the unsteady flow effects.

Table 2. Comparison of the numerical results with experimental data

	R_T , N (STAR CCM+)			R_T , N (EXP)
Cells, million	2.2 (M1)	3.4 (M2)	5.2 (M3)	
F_n				
0.073	9.415	11.079	10.757	10.767
0.099	17.664	18.127	18.071	18.338
0.135	31.931	32.367	31.309	31.294

Table 3. Relative error of the numerical results

Cells, million	Relative error, %		
	2.2 (M1)	3.4 (M2)	5.2 (M3)
F_n			
0.073	-12.550	2.90	-0.08
0.099	-3.672	-1.15	-1.46
0.135	2.037	3.43	0.05

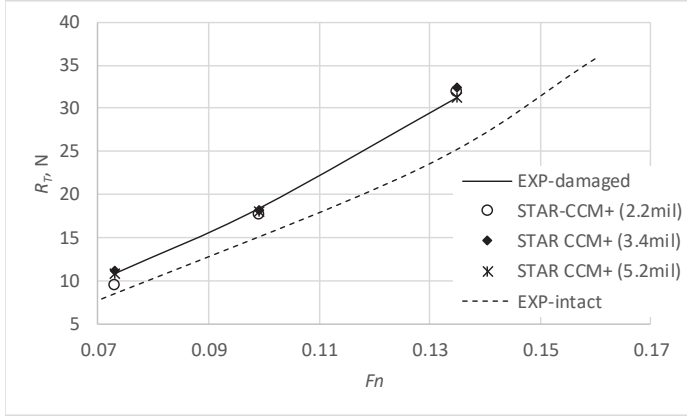


Fig. 8 Comparison of the numerical results with experimental data

An increase in the total resistance force of the damaged tanker model due to the presence of the flooded tank is about 25%. Since the draught of the damaged tanker model increased by over 5% after the flooding of the compartment of the model in the intact condition, a large part of this total resistance increase is due to larger frictional resistance for the larger wetted surface area. For Froude number 0.135, 7.9% of the total resistance force acts on the tank walls. Considering the large amount of flooded water inside the tanks and the unsteady flow effects that occur, it would be beneficial to determine the influence of sloshing on the global ship motions. The total resistance increase is mainly due to larger frictional resistance on the ship model hull.

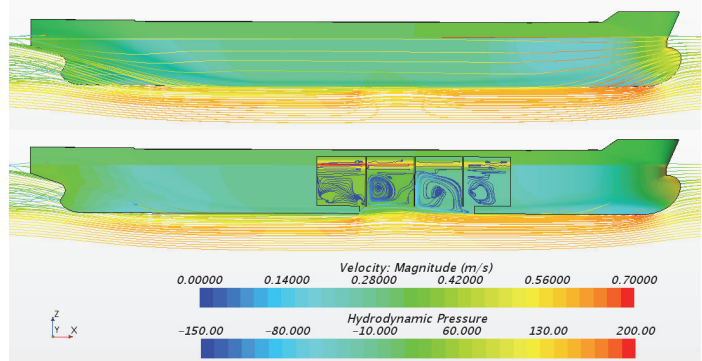


Fig. 8 Hydrodynamic pressure and streamlines around the hull and inside the tank on the symmetry plane for $F_n=0.073$

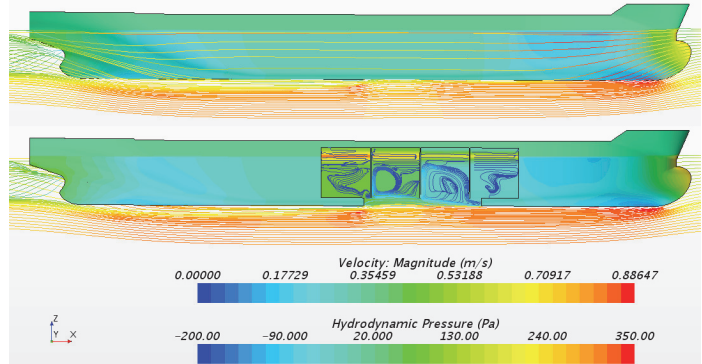


Fig. 9 Hydrodynamic pressure and streamlines around the hull and inside the tank on the symmetry plane for $F_n=0.099$

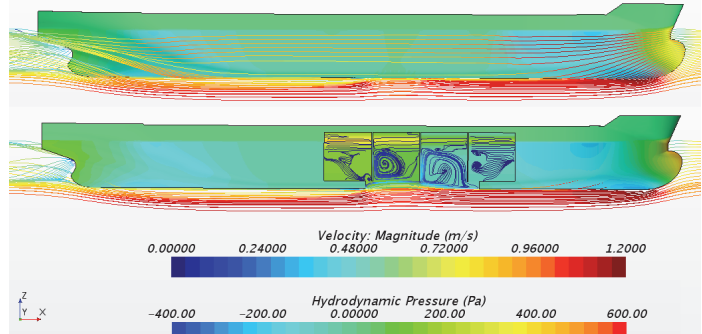


Fig. 10 Hydrodynamic pressure and streamlines around the hull and inside the tank on the symmetry plane for $F_n=0.135$

The obtained hydrodynamic pressure, as well as the streamlines inside the tank and around the hull, can be seen in Figs. 8~10 for all considered Froude numbers. Flow inside the tanks advects very slowly for all considered Froude numbers, especially in the first and last tank which can be seen from the obtained magnitude of the velocity from the streamlines. However, due to transversal bulkheads, especially those located in the positions of frames #112 and #128, flow circulation occurs inside the two middle tanks.

As the model speed increases, the circulation velocity of flow inside the tanks reaches higher values while the flow velocity in the first and last tank remains relatively low. The free surface inside the tank obtained using the VOF method is shown in Figs. 11~13. As can be seen, relatively low disturbance of the free surface is obtained for all considered Froude numbers.

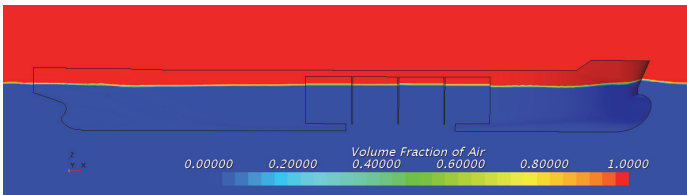


Fig. 11 Free surface inside the tank obtained by the VOF method using coarse mesh M1 for $F_n=0.135$

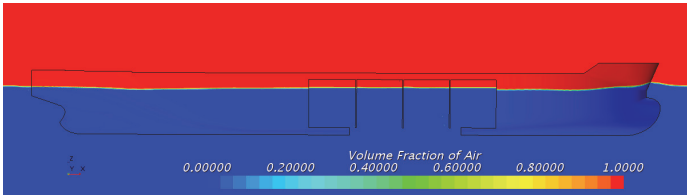


Fig. 12 Free surface inside the tank obtained by the VOF method using medium mesh M2 for $F_n=0.135$

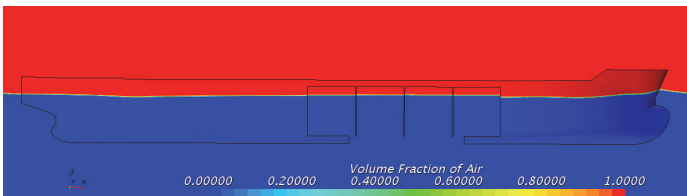


Fig. 13 Free surface inside the tank obtained by the VOF method using fine mesh M3 for $F_n=0.135$

CONCLUSIONS

In this paper, the total resistance force of the tanker model with eight flooded compartments in calm water was numerically obtained using the commercial RANS solver STAR-CCM+ and compared to the experimental data. CFD tools based on viscous flow can be successfully used in modelling the fluid flow around the ship hull and the complex flow inside the flooded tanks. The aim of this research was to investigate the mesh sensitivity of the obtained results and to validate RANS FVM for the prediction of the total resistance force of the damaged hull, which is necessary for the proper organization of damaged tanker salvage operations. Three different mesh densities were created, and only the finest mesh provided steady resistance force while the coarse and medium mesh led to some convergence issues. In order to achieve the numerical convergence of the results considering the complex non-linear flow phenomenon inside the tanks, high mesh density should be used. The numerical results obtained using fine mesh show good agreement with the experimental data and the oscillating results using the other two meshes were averaged. The sharp edges of the geometry of the damage hole and transverse bulkheads led to high pressure gradients in these areas, and unsteady flow effects occurred, which resulted in an unsteady total resistance force for all considered Froude numbers. The average resistance increase compared to the total resistance force of the intact model is mainly due to the larger wetted surface area and larger frictional resistance. However, due to an increased inflow velocity and higher circulation inside the tanks that are fully open to the seaway, it could also be beneficial to investigate the global motions of the damaged model coupled with fluid motions inside the tanks, especially at higher model speeds. This will form part of future work, as will an investigation of the effect of the turbulence model and time step on the total resistance force of the damaged model.

ACKNOWLEDGEMENTS

This study has been supported in part by the Croatian Science Foundation under project 8658 and by the University of Zagreb, Faculty of Mechanical Engineering and Naval Architecture.

REFERENCES

- Bašić, J, Degiuli, N, Dejhalla, R, (2017). "Total resistance prediction of an intact and damaged tanker with flooded tanks in calm water," *Ocean Engineering*, 130, 83-91.
- Brodarski Institute, 2015. Report 6454-M. Tech. rep., Brodarski Institute, Zagreb.
- CD Adapco, (2016). Tutorial Guide for STAR-CCM+ 11.02.010-R8.
- Farkas, A, (2016). *Numerička simulacija viskoznog strujanja oko trupa broda*, Master Thesis, Zagreb, Croatia.
- Ferziger, JH, Perić, M (2002). *Computational Methods for Fluid Dynamics*, (Third Edit.), Springer, Berlin, Germany.
- Gao, Z, Gao, Q, Vassalos, D (2011). "Numerical simulation of flooding of a damaged ship," *Ocean Engineering*, 38, 1649-1662.
- Gao, Z, Vassalos, D, Gao, Q (2009). "A Multiphase CFD Method for Prediction of Floodwater Dynamics," *STAB 2009: 10th International Conference on Stability of Ships and Ocean Vehicles*, St Petersburg, Russia, 307-316.
- Guo, BJ, Deng, GB, Steen, S (2013). "Verification and validation of numerical calculation of ship resistance and flow field of a large tanker," *Ships and Offshore Structures*, 8(1), 3-14.
- Lee, S, You, JM, Lee, HH, Lim, T, Park, ST, Seo, J, Rhee, SH, Rhee, KP (2016). "Experimental Study on the Six Degree-of-Freedom Motions of a Damaged Ship Floating in Regular Waves," *IEEE Journal of Oceanic Engineering*, 41(1), 40-49.
- Lee, S, You, JM, Lee, HH, Lim, T, Rhee, SH, Rhee, KP (2012). "Preliminary tests of a damaged ship for CFD validation," *International Journal of Naval Architecture and Ocean Engineering*, 4(2), 172-181.
- Marine Environment Protection Committee, (2003). *Resolution MEPC.110(49) - Revised interim guidelines for the approval of alternative methods of design and construction of oil tankers under Regulation 13F(5) of Annex I of MARPOL 73/78*.
- Querard, A.B.G., Temarel, P., Turnock, S.R. (2008). "Influence of viscous effects on the hydrodynamics of ship-like sections undergoing symmetric and anti-symmetric motions, using RANS," *Proceedings of the ASME 27th International Conference on Offshore Mechanics and Arctic Engineering (OMAE)*, Estoril, Portugal, 1-10.
- Wood, CD, Hudson, DA, Tan, M (2010). "CFD Simulation of Orifice Flow for the Flooding of Damaged Ships," *Proceedings of the 3th Numerical Towing Tank Symposium*, Duisburg, Germany, 144-149.
- Yang, J, Rhee, SH, Kim, H, (2009). "Propulsive performance of a tanker hull form in damaged conditions," *Ocean Engineering*, 36(2), 133-144.